Modelling and Evaluating Optical Transmission with the OCATA Optical Time Domain Digital Twin

Luis Velasco
Advanced Broadband Communications Center (CCABA)
Universitat Politecnica de Catalunya (UPC) Barcelona, Spain
email: luis.velasco@upc.edu

Marc Ruiz
Advanced Broadband Communications Center (CCABA)
Universitat Politecnica de Catalunya (UPC) Barcelona, Spain
email: marc.ruiz-ramirez@upc.edu

***Abstract*—We review the basis of the OCATA digital twin, including the information that can be extracted from IQ optical constellations, how optical time-domain propagation can be modelled using Deep Neural Networks, and tuned from telemetry data. We cover from single channel to multiple sub-carrier signals and multi-band optical transmission. Applications of OCATA are afterward reviewed, including accurate quality of transmission (QoT) estimation and nonlinear noise mitigation.**

Keywords—Optical digital twin, QoT estimation, nonlinear noise mitigation

I. Introduction

Digital twins, working together with software-defined networking (SDN) control, have shown their potential for a wide range of applications related to the operation of optical networks, including Quality of Transmission (QoT) estimation for optical connection provisioning and failure management. In this paper, we provide an overview of the OCATA optical time domain digital twin first proposed in [1], [2] and extended to support not only single carrier (SC) in the optical C-band, but also digital subcarrier multiplexing (DSCM) [3] and optical multiband (MB) transmission [4], as well as to show its applications for QoT estimation and efficient failure management [5].

OCATA models the propagation of the optical signal in the time domain. Specifically, OCATA includes Deep Neural Networks (DNN) that model how in-phase (I) and quadrature (Q) constellations are impaired by linear (LI) and nonlinear (NLI) noise when propagating through the optical components, i.e., Reconfigurable Optical Add-Drop Multiplexers (ROADM) and optical links, defined by a lightpath. Because network digital twins largely rely on telemetry data, received IQ constellations need to be collected from the optical transponders (TP). However, due to the large size of the measured data, compression techniques have been proposed to reduce bandwidth requirements [6].

The rest of the paper is organized as follows. Section II introduces the rationale behind analyzing optical IQ constellations and the OCATA approach for modelling signal propagation along a lightpath. The general architecture for the control plane and an example for SC optical transmission are also introduced. Next, in Section III, extensions to OCATA are presented, including our approach to improve the lightpath models with telemetry data, as well as the support for DSCM signals and MB optical transmission. Illustrative results are presented in Section IV, where QoT estimation from OCATA is compared with actual QoT based on both synthetic and experimental data, available in [7]-[10]. Finally, Section V draws the main conclusions of this work.

The research leading to these results has received funding from the European Union's Horizon Europe research and innovation programme SEASON (G.A. 101096120) project and from the ICREA institution.

II. OCATA Digital Twin

In this section, we assume that SC signals are generated at TP A and transmitted in the optical C-band to TP B, along a give lightpath. Fig. 1a presents an illustrative scenario with a lightpath connecting two end locations equipped with TP A and TP B through an optical network consisting of several ROADMs and optical links. Every ROADM includes Wavelength Selective Switches (WSS) and optical amplifiers (OA), whereas every optical link is composed of OAs and single mode optical fiber spans. TP nodes and ROADMs are controlled by a local node agent that configures the underlying optical devices and collects telemetry measurements from them.

On top of the architecture, an SDN controller connects to the node agents for network programmability and measurements collection [6]. In addition, OCATA digital twin connects to the SDN controller and includes (or it has access to): *i*) a telemetry database (DB), where collected measurements are stored; *ii*) a model DB that includes models for several purposes ranging from physical layer to QoT estimation and failure identification; *iii*) a sandbox domain that is used for composing models representing lightpaths or for offline training of ML models. Training datasets in the sandbox can be populated initially based on the results from simulations and lab experiments, and then from the received telemetry measurements. They can also be augmented to include not-yet-considered patterns (e.g., related to soft-failures), which are added as soon as they are detected (see [11]); and *iv*) a set of algorithms that are used to analyze the measurements received, e.g., for QoT estimation, compare the signals to those generated by the models, and apply nonlinear noise mitigation.

The next subsections introduce the main concepts and functionalities of OCATA, from modelling to QoT estimation.

A. Lightpaths modeling based on components DNN models

In OCATA, DNNs have been trained to model the propagation of the signal on the optical components, so lightpath models can be built as a concatenation of DNN-based component models. In particular, incoming optical signals using *m*-Quadrature Amplitude Modulation (QAM) format are processed in the time domain. Therefore, DNN models use as input a set of features Y_i characterizing every constellation point (CP) *i*: 1..*m*. CPs are assumed to follow bi-variate Gaussian distributions, so each vector Y_i includes 5 features representing the real and imaginary mean position in the constellation (μ) and the real and imaginary variance and

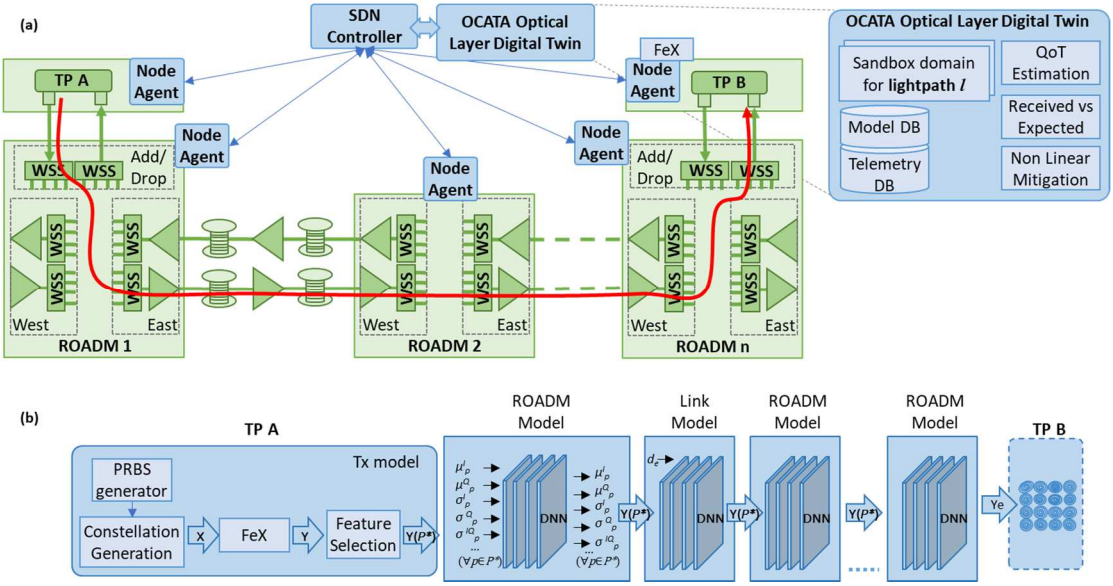

Fig. 1. Overview of the optical network scenario (a). Modelling a lightpath by concatenating DNN components models (b).

symmetric covariance terms (σ), i.e., $Y_i = [\mu^I,\mu^Q,\sigma^I,\sigma^Q,\sigma^{IQ}]_i$. In addition, DNN modes for optical links need an input with the accumulated distance that the signal has traversed from the Tx to the start of the link.

Because DNNs are pre-trained, the concatenated DNN representing the signal propagation through the lightpath can be very quicky composed by selecting individual DNN models from a repository. Such propagation increases the LI and NLI noise resulting in higher values for σ^I and σ^Q at the output of the DNNs, which can be related to QoT-related indicators. The concatenation model abstracting the lightpath in Fig. 1a is presented in Fig. 1b. In this case, the signal crosses n ROADMs and n-1 optical links each with different length and number of spans. ROADMs are modelled as two WSS, and every intermediate ROADM, except the last one before the Rx (drop), includes a booster OA that compensates for WSSs insertion losses. Typically, the insertion losses in the last ROADM are compensated by DSP techniques at the digital coherent Rx. The optical links consist of fiber spans and inline OAs that compensate for the losses of the fiber spans. We assume that the pre-OA at ROADM's input is a part of the link model.

Models for both ROADM and link components follow a similar architecture. Those models propagate feature set Y, modifying the mean and variance of each CP according to the LI and NLI noise that the physical element introduces. For scalability reasons, the DNN models consider the propagation of the features for a subset of selected CPs P^* only. Specifically, two exterior and two interior CPs are selected as representative of the impact of noise during propagation, whereas the rest can be generated as a function of the propagated CPs. Hence, the features in Y that belong to constellation point subset P^*, denoted as $Y(P^*)$, are selected.

Then, this reduced set of features is propagated through a DNN model specifically trained for the component that is represented. The structure of the DNN consists in $5\cdot|P^*|$ input and output features (i.e., μ and σ vectors of the selected CPs), and a number of hidden layers with variable number of hidden neurons each.

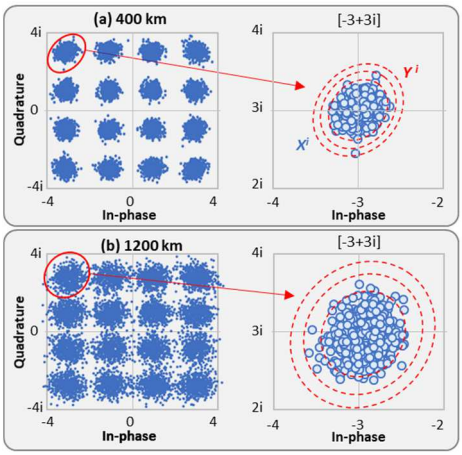

Fig. 2. GMM fitting for feature extraction (Fex).

Finally, the Tx model generates the initial feature set Y. A pseudo-random bit sequence (PRBS) generator generates the bit sequence that is used to produce the initial IQ optical constellation following a Tx configuration. Such initial constellation can be generated using analytical equations, simulation, ML models, etc. The IQ optical constellation (X) consist of a set of symbols $x \in X$, where each $x=[x^I, x^Q]$ belongs to a CP. Once the initial optical constellation is generated, a *feature extraction* block computes the supervised features Y from the IQ constellation described by X.

B. *Feature Extraction (FeX)*

As previously defined, the Feature Extraction (FeX) block takes as input IQ constellations, denoted X, and produces feature set Y. IQ constellation are defined by a sequence of complex symbols $x \in X$, where the real and imaginary parts represent the I and Q components of the optical signal, respectively. In an m-QAM optical signal, every symbol belongs to one of the m possible CPs.

Because we assume that each CP follows a Gaussian distribution, FeX uses Gaussian Mixture Models (GMM) to characterize X as a set of m bivariate Gaussian distributions. In the example in Fig. 2, GMM fitting has been applied to

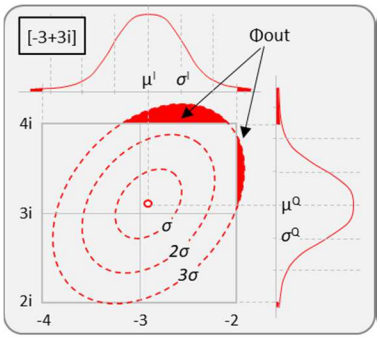

Fig. 3. Example of Φ_{out} feature for constellation point [-3+3i]

characterize the constellation point [-3+3i] of an m=16 QAM optical signal after transmission along 400 and 1200 km. Then, for every input sample X, a set of semi-supervised constellation features Y that characterizes X is generated. In particular, FeX uses GMM fitting to characterize every CP i by means of vector Y_i, as previously introduced. It is worth noting that the dispersion of symbols that belong to a certain CP provides valuable insight of the level of noise affecting the signal, both LI and NLI noise. As the total noise increases, the dispersion of the symbols also increases. This fact also makes constellation characterization more challenging.

FeX is used whenever an IQ constellation needs to be processed by OCATA, including those real ones measured by the Rx, as depicted in Fig. 1a, where constellations are processed at the node agent.

C. Comparing received and expected signals

As illustrated in Fig. 1b, OCATA can be used to generate the features Y_e that represent the signal X_e that is expected at the Rx side crossing the optical components defined by a specific lightpath. Such expected signal can be compared to the real signal at the Rx, denoted X_r. Function $diff(X_r, X_e)$ (1) can be used to compare both signals; it computes the Euclidean distance of the difference between the features extracted from X_r and the expected ones, i.e., Y_e.

$$diff_Y(X_r, X_e) = \|Y_r - Y_e\|_2 \quad (1)$$

Application cases for (1) include model tuning with telemetry measurements, as well as failure detection. In both cases, the received signal is compared to the one predicted by the lightpath' model and used to improve the model or for the early detection of degradations. Specifically, the analysis of the evolution of degradation in time can be captured, monitored and analyzed to find the root cause of such degradation in the time domain, which greatly complements the frequency domain analysis in [12]-[14].

D. QoT estimation

The basic features Y defined in the previous subsections can be used to estimate the QoT of the signal in a meaningful range. Note that Y characterizes the scattering of symbols around their mean using bivariate Gaussian distributions and, in turn, such scattering is related to the Symbol Error Rate (SER) of the signal. Nevertheless, the characterization of Y and its relationship with the BER is not trivial. In view of that, a new feature, denoted Φ^i_{out}, is added to compute the probability that a symbol initially transmitted in CP i is detected at the receiver out of the detection area of such CP, denoted as A^i.

Fig. 3a shows an example of Φ^i_{out} feature for constellation point [-3+3i]. The contours represent the different levels of the bi-variate Gaussian distribution that characterize this CP for a given lightpath. For the sake of clarity, we depict σ, 2σ, and 3σ levels only; univariate marginal distributions are provided for both I and Q axes. The area highlighted in red in both bi-variate and marginal distributions represents the region that falls out of A^i, i.e., the square delimited by vertices [-4+4i] and [-2+2i]. Hence, Φ^i_{out} is formally defined in (2)-(3).

$$\Phi^i_{out} = 1 - \phi_A(i) \quad (2)$$

$$\phi_A(i) = P\left(x \subset A^i \middle| x \sim N(Y^i)\right) \quad (3)$$

$$\text{(pre-FEC) BER} \sim \frac{\Phi^{avg}_{out}}{\log_2(m)} \quad (4)$$

$$\text{Q-factor [dB]} = 20 \cdot \log_{10}\left(\sqrt{2} \cdot \text{erfc}^{-1}(2 \cdot \text{BER})\right) \quad (5)$$

The pre-FEC BER can be estimated from Φ^i_{out} as defined in (4), where Φ^{avg}_{out} is the average Φ^i_{out} among the CPs. Φ^{avg}_{out} is interpreted as an estimation of the SER, so pre-FEC BER is derived assuming that 1 symbol error causes only 1 bit error (which is reasonable when employing Gray coding). Finally, (5) can be used to derive the Q-factor from the pre-FEC BER when the optical signals are perturbed by additive white Gaussian noise, where $erfc^{-1}$ is the inverse complementary error function.

III. Extending OCATA

In this section, we first introduce how concatenated DNN models can be tuned with telemetry data and how the dimensionality of that data can be reduced [6]. Then extensions of OCATA to support DSCM, summarized from [3], and MB transmission, from [4], are presented.

A. Improving Lightpath DNN Models with Telemetry

The features Y, generated by the Tx model in Fig. 1b, are propagated through the DNN that results from concatenating individual DNNs modelling the different optical components (ROADMs and optical links) along the path. As introduced in Section II, such models are pretrained with data from different sources, e.g., simulations, experiments, etc. and the resulting DNNs are stored in the model DB in OCATA (see Fig. 1a). Even though the DNN models are trained with high precision, the concatenated DNN can present imperfections because of the accumulated error and variation with the time of the behavior optical devices, e.g., the noise figure on the OAs, new splices in the fiber, etc. For this very reason, the concatenated DNN models require to be tuned periodically, from the monitoring measurements collected from the transponders. Tuning concatenated DNNs (Fig. 4) consists in applying Bayesian hyperparameter optimization (HPO) to build a probabilistic model of the function mapping hyperparameter values to the objective. Specifically, we target at minimizing the average $diff(X_r, X_e)$ (1), where X_r is the signal as measured at the Rx, evaluated with 5-fold cross evaluation. By iteratively evaluating promising hyperparameters (e.g., learning rate, architecture, activation function, and optimization algorithm), HPO finds a tuple of hyperparameters that yields an optimal model, which minimizes the $diff(\cdot)$ function.

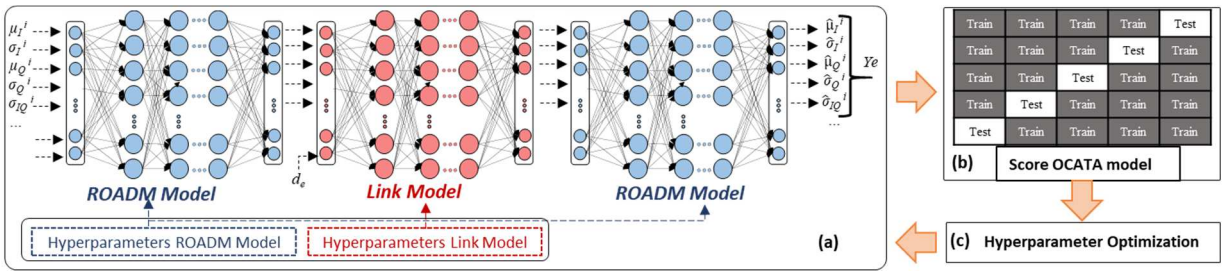

Fig. 4. Hyperparameter optimization of the lightpath concatenated DNN in OCATA.

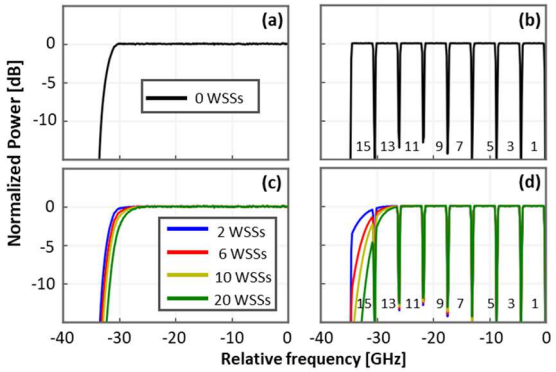

Fig. 5. Optical spectra of SC (a, c) and DSCM signals (b, d) at the Tx (top) and after cascaded WSSs (bottom).

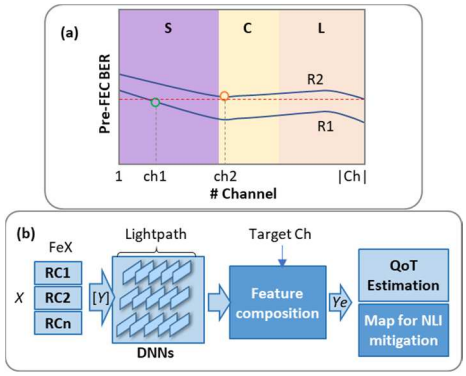

Fig. 6. Main building blocks of the OCATA-MB time-domain digital twin.

Because every sample X_r might include a large number of symbols, i.e., complex numbers, in addition to use FeX to extract the features Y_r from the collected sample X_r *autoencoders* (AE) can be used for intelligent IQ constellations compression. The proposed AEs run in the local node where the IQ constellations X_r are collected from the TP and encodes them into latent space $Z=[z_1, \ldots, z_L]$, typically of a size significantly lower than that of X. Then, Z can be conveyed to the centralized location where OCATA runs, where a decoder reconstructs the original data back.

B. DSCM Signals

When compared to SC, DSCM signals are more robust against the NLI noise as in general they work in the NLI "sweet spot" in terms of symbol rate (SR), i.e., from 4 GBd to 16 GBd per digital subcarrier (DSC). Even though the impact of the NLI noise is low, which leads to a mid-to-low performance penalty, other impairments (e.g., filtering distortions arising from the narrowing of the filter transmission bandwidth) play a critical role. For illustrative purposes, let us revisit the scenario in Fig. 1 and study the differences between SC and DSCM. Fig. 5 shows the spectrum after TP A and the spectra after traversing several ROADMs for a SC signal (Fig. 5a,c) and a 16-subcarrier DSCM signal (Fig. 5b,d). As expected, the outer DSCs exhibit larger filtering penalties compared to the inner ones, which becomes more evident as the number of cascading filters increases. If the equivalent bandwidth of the filtering cascade is reduced by a value larger than the bandwidth of an individual DSC, then the edge DSC will be completely filtered out. On the other hand, the inner DSCs are mostly unaffected and can be used for reliable data transmission even after several WSSs. In summary, filter cascading impacts differently SC and DSCM signals; while the whole SC signal degrades by filtering penalties, only external DSCs are degraded in DSCM transmission.

In view of the above, it is important to provide differentiated models for the transmission of different DSCs, particularly for propagation through ROADMs. For this very reason, specific DNN models have been considered depending on the DSC: *i*) for the two *outer* DSCs (i.e., DSCs 15 and 16); *ii*) the two *intermediate* DSCs 13 and 14; *iii*) for the *inner* DSCs (i.e., DSCs from 1 to 12); and *iv*) for the SC signal.

C. MB Optical Transmission

The classical OCATA architecture for C-band in Fig. 1b considers that DNN models are independent of the specific channel; a reference channel (RCh) in the middle of the C-band is assumed. DNNs are pre-trained for the RCh, so the concatenated DNN representing the signal propagation can be very quickly composed by selecting individual DNN models from the model DB.

However, in MB optical transmission, the inter-channel stimulated Raman scattering (ISRS) effect increases the impact of fiber nonlinearities by transferring power from higher to lower frequencies, which impacts the QoT of lightpaths using the different channels in a nonidentical manner. To illustrate such differentiated QoT, Fig. 6a shows the pre-FEC BER that an optical connection using a given route on the optical network would experience when the different channels are used. Two routes (R1 and R2) are considered with different total lengths, being R2 longer than R1. In general, we observe that the channels in the S band are more impacted for the same route and therefore, they can support shorter optical connections, as compared with the channels in the C and L bands.

As a result, the OCATA architecture for the C-band, needs to be updated so DNN models are pretrained for specific channels (or ranges), which would highly increase the number of DNNs to be managed. To avoid the explosion of DNN models, the architecture of OCATA MB (see Fig. 6b)

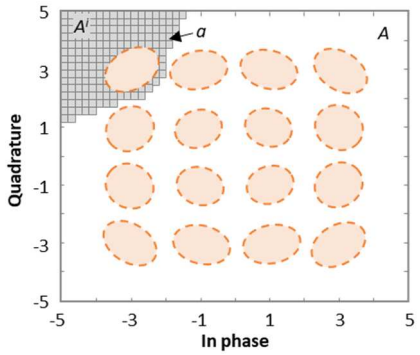

Fig. 7. Definition grid for 16-QAM signal constellations.

Algorithm 1. Compute Detection Areas

INPUT: Y, A, m **OUTPUT:** $[A^i]$

$A^i \leftarrow \emptyset$, **for each** i:1..m
  for each a in A **do**
    a.i $\leftarrow$ 0; a.maxProb $\leftarrow$ 0
    for i: 1..m **do**
      if $\varphi_a(i) > a$.maxProb **then**
        a.maxProb $\leftarrow \varphi_a(i)$; see (6)
        a.i $\leftarrow i$
    $A^{a.i} \leftarrow A^{a.i} \cup a$
  return $[A^i]$

considers a few RChs representing the specifics of different areas in the spectrum. Because OCATA models CP features propagation, the RChs are selected based on the different behavior of such features for selected CPs. However, the target channel might not be one of the selected RChs. Therefore, OCATA MB includes the Feature Composition block to estimate the CP features for any channel in the C+L+S bands based on the output of the DNN models propagating the features of the RChs. The algorithm for feature composition uses the features of the two adjacent RChs to the target channel to linearly interpolate the features $[Y^{i,ch}]$ for that channel. The output of the Feature Composition block can then be used for QoT estimation.

One functionality of OCATA that is important for MB transmission is that of the possibility to compute optimal detection areas to implement nonlinear noise mitigation in the Rx. Such functionality allows to improve the QoT of those optical connections with channel assignments providing poor QoT that would otherwise be blocked.

The method is based on dividing the whole coordinate IQ plane (A) into k small square areas a to create a grid. Fig. 7 shows an example for a 16-QAM signal, where A is defined by corner points [5+5i] and [-5-5i]. The detection area for CP [3+3i] is shown as a set of small areas. Then, the probability of receiving a symbol originally transmitted in CP i can be defined as (6), which facilitates computing Φ_A as (7).

$$\varphi_a(i) = P(x \subset a | x \sim N(Y^i)) \quad (6)$$

$$\phi_A(i) = \sum_{a \in A^i} \varphi_a(i) \quad (7)$$

With these definitions, the proposed method consists in assigning each of the small areas a to the detection area A^i of the CP i with the highest probability. Algorithm 1 shows the pseudocode of the algorithm that receives features Y, the coordinate plane A divided into small areas, and the number m of CPs in the signal, and computes a vector of detection areas $[A^i]$, where each area defines a subset of small areas of the whole coordinate plane. Vector $[A^i]$ can be then transformed into a map, so the Rx can easily decode the received symbols.

IV. Illustrative Results

This section evaluates OCATA for SC and DSCM optical signals. For evaluation, both synthetic and experimental data have been used and it is openly available in [7]-[10].

For generating realistic synthetic IQ constellations under different physical path characteristics, a simulator of a digital coherent system was implemented in MATLAB. Specifically: *i*) for SC signals in the C-band, we assumed a 16QAM@64GBd signal; *ii*) for DSCM, the signal is composed of 16 DSCs @4GBd spaced with a guard-band of 100 MHz. Modulation formats (MF) include 64QAM, 16QAM and QPSK; and *iii*) for MB optical transmission, we focused on 16QAM@32GBd signals and considered a C+L+S scenario with full spectrum usage, leading to 337 channels with 50 GHz channel spacing. Ranges of channels for the S, C and L bands are [1-128], [129-215], [216-337]. Signal samples are generated at the Tx side and shaped by a root-raised cosine filter with a 0.06 roll-off-factor assuming 100 GHz channel spacing. Then, the signal is propagated through standard single mode fiber spans, characterized by optimal power of -1 dBm, attenuation factor of 0.21 dB/km, dispersion parameter of 16.8 ps/nm/km, and nonlinear parameter of 1.14 1/W/km. Spans are modeled by solving the nonlinear Schrödinger equation using the well-known split-step Fourier method, whereas ideal inline OAs with a noise figure of 4.5 dB introduce LI noise. Specifically, OAs are modelled as EDFA for the C and L bands and thulium-doped fiber amplifier (TDFA) for the S band. Finally, a DSP block is considered at the Rx able to perform ideal chromatic dispersion compensation and phase recovery.

We start by validating the proposed BER estimation procedure based on the features Φ_{out}. For illustrative purposes, Fig. 8 shows the pre-FEC BER values obtained experimentally and through simulations as a function of Φ^1_{out} feature for constellation point 1 ([-3+3i]). Interestingly, we observe a clear correlation between both the pre-FEC BER in a logarithmic scale (SNR in dB) and the logarithm of Φ^i_{out} both for the synthetic and experimental lightpath configurations.

Let us now evaluate the extensions of OCATA for DSCM signals. Fig 9 shows the actual Q-factor for DSCs and SC signals with different MF versus the median and the min max range of the OCATA predicted ones. In this case, the Q-factor is used for comparison. Note that the predictions are less accurate in the case of DSCM, especially for the external subcarrier (i.e., DSC15), where the optical signal is affected by the most severe filtering penalties.

Finally, let us focus on MB optical transmission. For illustrative purposes, Fig. 10 shows the optimized detection areas for a lightpath with 6 spans using channels 1, 150 and 337. We observe the different shapes of the detection areas for the different channels. In Fig. 11, we observe that the maximum transmission distance is highly dependent on the selected channel, which stresses the application of OCATA-MB during lightpath provisioning to select a channel that can ensure that the FEC threshold is not exceeded. In addition, by configuring the optimal detection areas in the Rx, the maximum achievable transmission distance is effectively

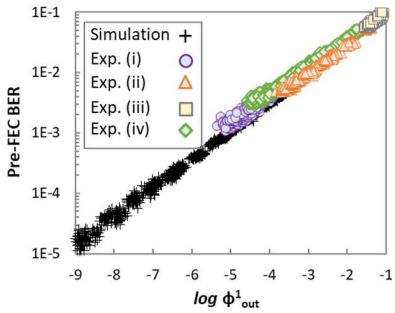

Fig. 8. pre-FEC BER vs. Φ_{out}.

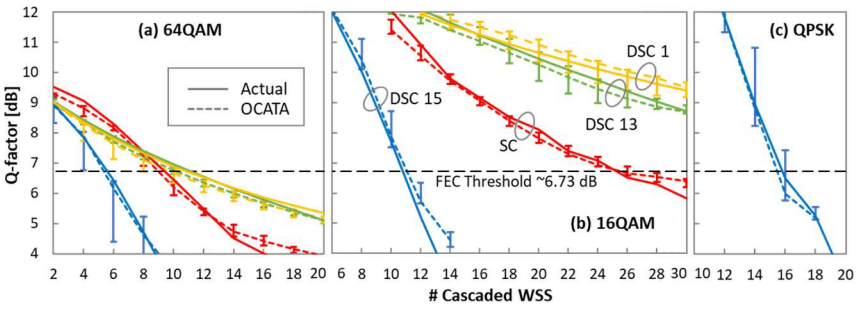

Fig 9. Actual vs OCATA predicted Q-factor for SC and DSCM.

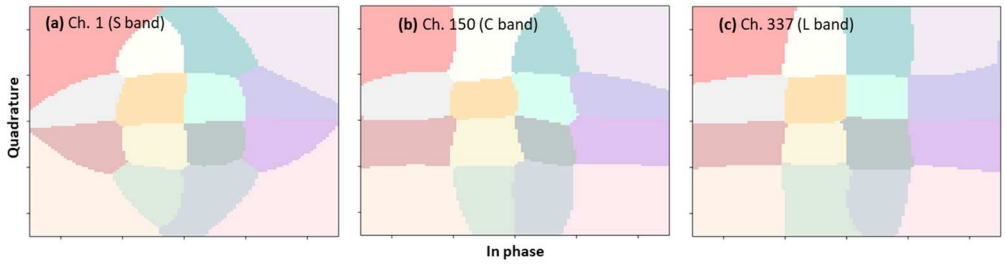

Fig. 10. Example of optimal detection areas (k=10,000) for 5 spans.

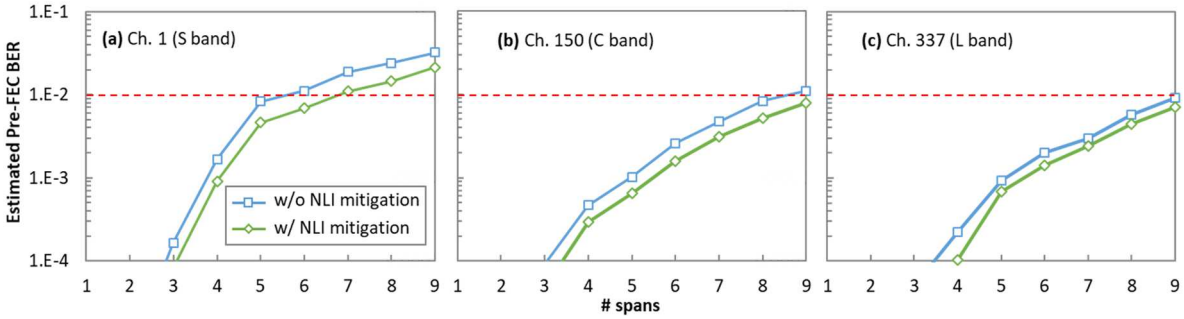

Fig. 11. Estimated pre-FEC BER with squared and optimized detection areas vs # spans.

extended. For instance, the reach of channel 1 can be extended by 1 additional span without exceeding the FEC threshold when nonlinear mitigation is implemented. Similar conclusions can be drawn for the other channels.

V. Conclusions

An overview of the main characteristics and extensions of the OCATA optical time domain digital twin have been presented. OCATA models optical signal propagation through optical components as DNNs. Such component DNNs can be concatenated to model optical signal propagation thought a lightpath. Although several applications of OCATA have been proposed so far, in this paper, we have concentrated on QoT estimation, as it can be used during lightpath provisioning, as well as for failure management. OCATA modelling of SC optical transmission in the C-band was extended for DSCM signals and MB optical transmission. Fine tuning of lightpaths DNNs based on telemetry data has been also covered.

Illustrative results of QoT estimation for different scenarios and using both synthetic and experimental data have shown the remarkable accuracy of OCATA.

References

[1] M. Ruiz, D. Sequeira, and L. Velasco, "Deep Learning -based Real-Time Analysis of Lightpath Optical Constellations," J. Opt. Comm. Netw., 2022.

[2] D. Sequeira *et al.*, "OCATA: A Deep Learning-based Digital Twin for the Optical Time Domain," J. Opt. Comm. Netw., 2023.

[3] M. Devigili *et al.*, "Twining Digital Subcarrier Multiplexed Optical Signals with OCATA for Lightpath Provisioning," J. Lightw. Techn., 2024.

[4] S. Ghasrizadeh *et al.*, "Digital Twin -Assisted Lightpath Provisioning and Nonlinear Mitigation in C+L+S Multiband Optical Networks," MDPI Sensors, vol. 24, pp. 1-21, 2024.

[5] M. Devigili *et al.*, "Applications of the OCATA Time Domain Digital Twin: from QoT Estimation to Failure Management," J. Opt. Comm. Netw., 2024.

[6] L. Velasco, P. González, and M. Ruiz, "Distributed Intelligence for Pervasive Optical Network Telemetry," J. Opt. Comm. Netw., 2023.

[7] M. Ruiz *et al.*, "Simulation and experimental data of frequency domain and time domain optical signal measurements for optical network digital twins," CORA.Repositori de Dades de Recerca, 2024.

[8] M. Ruiz, L. Velasco, and D. Sequeira, "Optical Constellation Analysis (OCATA)", CORA.Repositori de Dades de Recerca, 2022.

[9] M. Devigili, M. Ruiz, L. Velasco, "Synthetic measurements of single carrier and digital subcarrier multiplexing optical signals," CORA.Repositori de Dades de Recerca, 2024.

[10] S. Ghasrizadeh, M. Ruiz, L. Velasco, "Modified detection areas of constellation points of 16QAM signals for nonlinear impairment mitigation," CORA.Repositori de Dades de Recerca, V1, 2024.

[11] L. Velasco, B. Shariati, F. Boitier, P. Layec, and M. Ruiz, "A Learning Life-Cycle to Speed-up Autonomic Optical Transmission and Networking Adoption," J. Opt. Comm. Netw., 2019.

[12] A. P. Vela *et al.*, "BER Degradation Detection and Failure Identification in Elastic Optical Networks", J. of Lightw. Techn., 2017.

[13] B. Shariati, M. Ruiz, J. Comellas, and L. Velasco, "Learning from the Optical Spectrum: Failure Detection and Identification," J. Lightw. Techn., 2019.

[14] S. Barzegar *et al.*, "Soft-Failure Detection, Localization, Identification, and Severity Prediction by Estimating QoT Model Input Parameters," Trans. Netw. Service Mngt., 2021.